On tidally induced shocks in accretion discs in close binary systems

Savonije, G.J.; Papaloizou, J.C.B.; Lin, D.N.C.

DOI
10.1093/mnras/268.1.13

Publication date
1994

Published in
Monthly Notices of the Royal Astronomical Society

Mon. Not. R. Astron. Soc. **268**, 13–28 (1994)

On tidally induced shocks in accretion discs in close binary systems

G. J. Savonije,[1] J. C. B. Papaloizou[2] and D. N. C. Lin[2,3]
[1] *Astronomical Institute 'Anton Pannekoek', University of Amsterdam and Centre for High Energy Astrophysics (CHEAF), Kruislaan 403, 1098 SJ Amsterdam, The Netherlands*
[2] *School of Mathematics, Queen Mary and Westfield College, Mile End Road, London E1 4NS*
[3] *Lick Observatory, Santa Cruz, CA 95064, USA*

Accepted 1993 October 26. Received 1993 August 23; in original form 1993 June 18

ABSTRACT
We present linear and non-linear calculations of the tidal interaction of an accretion disc in close binary systems with mass ratios of unity and one tenth. We consider characteristic Mach numbers of the Keplerian flow between 10 and 50 and both inviscid discs and discs with an internal shear viscosity. We calculate the angular momentum transfer between the disc and the companion star and indicate how the excited spiral density waves can be understood in terms of a linear tidal response calculation. In agreement with earlier work it is found that hot, extended discs with Mach numbers $\mathscr{M} \leq 10$, such as those in close binary T Tauri stars, are subject to strong tidal coupling with the companion star, whereby the disc loses a sufficient amount of angular momentum through shock dissipation to enable disc matter to accrete on to the central star. For cool discs with Mach numbers $\mathscr{M} \geq 25$, thought typical for discs in cataclysmic variable and X-ray binaries, however, the wavelength of the tidal response is much shorter than the length-scale of the tidal force so that the tidal interaction becomes inefficient and, although adequate to truncate the disc, it produces little wave-driven accretion on to the central star.

Key words: accretion, accretion discs – hydrodynamics – celestial mechanics, stellar dynamics – binaries: close.

1 INTRODUCTION

Accretion discs are common in interacting binary systems such as cataclysmic variables (Warner 1976), X-ray binaries and binary T Tauri stars (Mathieu 1992) and their evolution is regulated by angular momentum transfer processes (Lynden-Bell & Pringle 1974). It has been known for some time that accretion discs in close binary systems can lose angular momentum to an orbiting exterior companion through tidal interaction (Papaloizou & Pringle 1977; Lin & Pringle 1976). Work on the effects of satellites on Saturn's rings (Goldreich & Tremaine 1978; Shu 1984) and protoplanets in the early solar nebula (Papaloizou & Lin 1984) has shown that this tidal interaction can result in the excitation of waves which propagate into the disc. If the disc is inviscid, these waves can propagate over large distances before they dissipate. If the disc is non-self-gravitating the tidal waves can take the character of shock waves. Because the tidally excited spiral pattern rotates with the binary angular speed ω, which is smaller than the angular speed of the gas in the disc, it carries negative angular momentum. Dissipation in the shocks therefore leads to a loss of disc angular momentum and consequent accretion of disc matter. The companion star, which excited the negative angular momentum waves, gains this angular momentum.

This tidally induced angular momentum transport mechanism suggests an attractive alternative to the ad hoc assumption that disc evolution is driven by turbulent viscosity (Shakura & Sunyaev 1973). In order to evaluate the validity of such a scenario, Sawada, Matsuda & Hachisu (1986) carried out a series of numerical simulations of an inviscid accretion disc in a close binary system of unit mass ratio with low Mach numbers $\mathscr{M} \leq 10$, i.e. for small ratios $\mathscr{M}$ of Keplerian speed to characteristic sound speed in their disc material. In this limit, they found that tidally induced waves could indeed propagate to small disc radii such that a significant amount of angular momentum could be effectively transported outward over an extended region in the disc. This led the authors to suggest that disc accretion might occur as a consequence of tidally induced shock waves occurring in an otherwise inviscid disc. Spruit (1987, 1989) constructed a steady state, non-axisymmetric, self-similar disc model which involves a non-linear wave with zero pattern speed giving dissipation and angular momentum flow at shock discontinuities (see also Lubow & Shu 1975; Donner 1979; Larson 1990). Although the companion's tidal torque is not explicitly considered in the semi-analytic treatments, it must be thought of as ultimately responsible for the angular momentum flow out of the disc. Subsequent two-dimensional numerical simulations for disc models in which the characteristic sound speed is a significant fraction of the Keplerian speed, lead to results that seem compatible with these semi-analytic calculations (Sawada et al. 1987; Spruit et al. 1987; Różyczka & Spruit 1989; Matsuda et al. 1987, 1989; Spruit 1989).

These results were applied to the context of accretion disc flow in cataclysmic variables (Sawada et al. 1986). It is believed (Pringle 1981), however, that the effective Mach numbers in observed discs in cataclysmic variables are large (≥ 25). In these circumstances it has been argued that the response to tidal forcing will be considerably weakened relative to the low Mach number case (Lin & Papaloizou 1993). This is because the characteristic wavelength of the excited waves decreases with increasing Mach number, so that it becomes very small compared with the scale associated with the forcing potential. Further, from the observed spectral evolution of cataclysmic variables, modest values of the viscosity are inferred such that their values correspond to viscosity parameter $\alpha > 0.1$ (Pringle 1981). Under these conditions the waves could be dissipated by viscosity, rendering the shock waves ineffective, except possibly at large disc radii.

It is the purpose of this paper to investigate the tidal interaction and consequent excitation of waves in close binary systems with mass ratio unity and one tenth. We study this phenomenon as a function of disc size and Mach number. We take care that our calculations have adequate resolution to represent the shorter wavelength responses expected in the high Mach number cases. Because we are interested in non-self-gravitating discs with no internal shear viscosity there is no strictly steady state solution in which the removal of angular momentum due to tidal interaction balances the angular momentum transported outward through the action of shear viscosity. We therefore employ two-dimensional evolutionary calculations using finite difference schemes based on an Eulerian mesh rather than the Lagrangian scheme of Lin & Papaloizou (1986), which can be used only to find steady state solutions for viscous discs. We evolve discs forward in time until a slowly evolving quasi-steady state, rather than a strict steady state, is achieved. We do not find any evidence for episodic accretion in our calculations. We remark that, because the calculations are two-dimensional, there may be neglected effects in three dimensions which could inhibit the propagation of waves over large radial distances. Lin, Papaloizou & Savonije (1990a,b) found that the refraction of initially radially propagating wave-fronts due to a sound speed variation with height tends to make the propagation direction bend upwards. As mentioned by these authors, this effect is most important for waves with large azimuthal mode number m. Because these have short wavelengths and high frequencies, they are readily deflected to propagate over large distances vertically and are thus susceptible to suffering shock dissipation in an extended tenuous atmosphere. Linear waves with low m, which might be expected when the binary companion has a significant mass ratio, may be reflected as a result of the decreasing density gradient at relatively small heights and thus be able to propagate radially. But note that, if these waves become non-linear, their profiles necessarily distort and develop short wavelength components for which vertical propagation might be important. This indicates that effects which might hinder the inward propagation of waves may have been ignored. In this sense the tidal effects found here are to be regarded as an upper limit.

We will compare the tidal torque generated in the non-linear evolutionary calculations with those calculated from linear response calculations. The purpose of this approach is to confirm that the excited waves can be understood in terms of a linear response calculation of the type used in similar problems arising in Saturn's rings and the early solar nebula (see, for example, Goldreich & Tremaine 1980). The linear theory normally predicts that spiral waves are generated at Lindblad resonances in the disc. For the mass ratios and discs considered here there are no such resonances with their centres inside the disc. Nevertheless, the centre of the 2:1 resonance (where the disc angular speed $\Omega = 2\omega$) can be thought of as lying in the vicinity of the boundaries of the disc. Because the resonance has a finite width that increases with the magnitude of the sound speed, it can still generate a substantial wave-like spiral response in the disc. Our calculations indicate that, in large inviscid discs, wave generation can drive substantial accretion up to small disc radii only if the disc's Mach number is low (≤ 10). If the Mach number is significantly larger than this value, as is expected in observed discs in cataclysmic variables, wave excitation and propagation become ineffective and unable to reach small radii at significant amplitude, unless perhaps the surface density is very much reduced there. In addition, we have performed some calculations using a different method with viscosity included, and find that waves may be rapidly damped if a viscosity comparable to that required in realistic disc models is present in the disc.

A brief outline of this paper is as follows. In Section 2 we give the basic equations. In Section 3 we give the relevant parts of the theory of the linear response to tidal perturbations for inviscid discs, from which the angular momentum transfer rate between disc and binary companion is calculated. In Section 4 we describe our numerical methods and present our numerical non-linear results. Finally, in Section 5, we present our conclusions.

2 BASIC EQUATIONS

To describe the disc response to the tidal torque of a perturbing mass, we adopt a thin-disc approximation in which there is no vertical motion. We work in a non-rotating cylindrical coordinate system (r, ϕ, z) defined with the origin at the primary mass M with z being the vertical coordinate. We define Σ $(\equiv \int_{-\infty}^{\infty} \rho \, dz)$ and P $(\equiv \int_{-\infty}^{\infty} p \, dz)$ to be the surface density and vertically integrated pressure, respectively. The radial component of the equation of motion can be written

$$\frac{\partial v_r}{\partial t} + v_r \frac{\partial v_r}{\partial r} + \frac{v_\phi}{r} \frac{\partial v_r}{\partial \phi} - \frac{v_\phi^2}{r} = -\frac{1}{\Sigma} \frac{\partial P}{\partial r} - \frac{\partial (\Psi + \psi)}{\partial r} + \frac{1}{\Sigma} \frac{\partial}{\partial r}\left(\frac{4}{3} \nu_r \Sigma \frac{\partial v_r}{\partial r}\right), \tag{1}$$

where v_r and $v_\phi = r\Omega$ are the radial and azimuthal components of velocity, and Ψ and ψ are the gravitational potentials due to the primary point mass and the perturbing companion mass, respectively. We have also included the possibility of a radial viscous force with kinematic viscosity coefficient ν_r. The azimuthal component of the equation of motion in the flat-disc model is

$$\frac{\partial v_\phi}{\partial t} + \frac{v_\phi}{r}\frac{\partial v_\phi}{\partial \phi} + v_r\frac{\partial v_\phi}{\partial r} + \frac{v_\phi v_r}{r} = -\frac{1}{r\Sigma}\frac{\partial P}{\partial \phi} - \frac{1}{r}\frac{\partial \psi}{\partial \phi} + F_\nu, \tag{2}$$

where we allow for an azimuthal viscous force per unit mass

$$F_\nu = \frac{1}{\Sigma r^2}\frac{\partial}{\partial r}\left(\nu \Sigma r^3 \frac{\partial \Omega}{\partial r}\right),$$

ν being the shear viscosity. The perturbing gravitational potential due to a companion with mass M_s, orbiting with angular frequency ω, is

$$\psi = -\frac{GM_s}{[r^2 + D^2 - 2rD\cos(\phi - \omega t)]^{1/2}} + \frac{GM_s r\cos(\phi - \omega t)}{D^2}.$$

For a barotropic equation of state $P = P(\Sigma)$, the local sound speed, c, is a function of Σ with no additional explicit dependence on radius. It is defined through $c^2 = \mathrm{d}P/\mathrm{d}\Sigma$. Finally, the continuity equation reads

$$\frac{\partial \Sigma}{\partial t} + \frac{1}{r}\frac{\partial}{\partial r}(\Sigma r v_r) + \frac{1}{r^2}\frac{\partial}{\partial \phi}(\Sigma r v_\phi) = 0. \tag{3}$$

The main motion in the disc is rotation in the azimuthal direction and its angular frequency can be deduced from equation (1), in the limit of negligible v_r and ψ, such that

$$\frac{v_\phi^2}{r} = \Omega^2 r = \frac{1}{\Sigma_0}\frac{\mathrm{d}P_0}{\mathrm{d}r} + \frac{\mathrm{d}\Psi}{\mathrm{d}r},$$

where the subscript 0 denotes an unperturbed axisymmetric value. In the thin-disc limit, when the sound speed of the disc is very small, equation (2) gives $\Omega^2 \sim GM/r^3 \equiv \Omega_K^2$, which is just the Keplerian rotation law.

3 THE LINEAR RESPONSE OF THE DISC

Here we calculate the response of the disc after simplifying the governing equations by linearizing them. This problem has been considered by many authors in the context of planetary rings, galaxies and the early solar nebula (Goldreich & Tremaine 1978; Papaloizou & Lin 1984; Lin & Papaloizou 1986). In the applications considered above, the case when the mass of the orbiting companion is small has been considered. Waves are excited at Lindblad resonances which can be located in the disc in the low companion mass limit.

In this paper we consider the situation when the mass of the companion, which orbits outside the disc, is not small and there are no Lindblad resonances in the disc. In such cases, waves that carry negative angular momentum may still be excited due to the finite width of the resonance, albeit less effectively. But the process becomes less effective the lower the sound speed in the disc.

3.1 Linearization of the basic equations

We linearize equations (1) and (2), neglecting viscosity, such that

$$\frac{\partial v_r'}{\partial t} + \Omega\frac{\partial v_r'}{\partial \phi} - 2\Omega v_\phi' = -\frac{\partial}{\partial r}\left(\frac{\Sigma' c^2}{\Sigma_0}\right) - \frac{\partial \psi}{\partial r}, \tag{4}$$

and

$$\frac{\partial v_\phi'}{\partial t} + \Omega\frac{\partial v_\phi'}{\partial \phi} + \frac{v_r'}{r}\frac{\mathrm{d}(\Omega r^2)}{\mathrm{d}r} = -\frac{1}{r}\frac{\partial}{\partial \phi}\left(\frac{\Sigma' c^2}{\Sigma_0}\right) - \frac{1}{r}\frac{\partial \psi}{\partial \phi}. \tag{5}$$

In the above equations, perturbed quantities are denoted by a prime. In the unperturbed axisymmetric flow, $\Sigma = \Sigma_0$, $v_r = 0$ and $v_\phi = \Omega r$. The perturbed continuity equation is

$$\frac{\partial \Sigma'}{\partial t} + \Omega\frac{\partial \Sigma'}{\partial \phi} = -\frac{1}{r}\left[\frac{\partial}{\partial r}(r v_r' \Sigma_0) + \frac{\partial}{\partial \phi}(\Sigma_0 v_\phi')\right]. \tag{6}$$

There is a flux of angular momentum through a circle of constant radius r given by

$$F_H = \int_0^{2\pi} \Sigma_0 r^2 v_r' v_\phi' \, \mathrm{d}\phi. \tag{7}$$

To proceed further we expand ψ in a Fourier series in the azimuthal angle such that

$$\psi = \mathrm{Re}\left\{\sum_{m=0}^{\infty} W_m \exp[\mathrm{i}m(\phi - \omega t)]\right\}.$$

We consider situations where the companion, with mass ratio between 0.1 and 1, orbits outside the disc. Provided the disc outer boundary is not too close to the companion's orbit, the dominant contribution comes from the term with $m = 2$. Then, approximately (e.g. Savonije & Papaloizou 1983),

$$W_2 = -\frac{3}{4}\frac{GM_s}{D^3}r^2.$$

From now on we shall assume that terms corresponding to other values of m may be dropped, so that $m \equiv 2$. If we assume that all perturbations vary as $\exp[\mathrm{i}m(\phi - \omega t)]$, and take this factor as read, equations (4)–(6) give

$$\frac{1}{\Sigma_0 r}\frac{\mathrm{d}}{\mathrm{d}r}(\Sigma_0 r \xi_r) - \frac{2\Omega \xi_r}{r(\Omega - \omega)} = \left[\frac{K}{r^2(\Omega - \omega)^2} - \frac{K}{c^2}\right] + \frac{W_2}{r^2(\Omega - \omega)^2} \tag{8}$$

and

$$\frac{\mathrm{d}K}{\mathrm{d}r} + \frac{2\Omega K}{r(\Omega - \omega)} = \xi_r[m^2(\Omega - \omega)^2 - \Omega^2] - \frac{\mathrm{d}W_2}{\mathrm{d}r} - \frac{2\Omega W_2}{r(\Omega - \omega)}, \tag{9}$$

where $K = \Sigma' c^2/\Sigma_0$, and $\xi_r = [\mathrm{i}m(\Omega - \omega)]^{-1} v_r'$ is the Lagrangian displacement in the radial direction.

The above two linearized equations of motion, being a pair of first-order ordinary differential equations, require two boundary conditions. For a disc with outer boundary $r = R$ at which Σ_0 vanishes smoothly, we require the boundary condition

$$K=-\frac{\xi_r}{\Sigma_0}\frac{\mathrm{d}P_0}{\mathrm{d}r} \qquad (10)$$

to avoid a singularity at $r=R$. But note that a rigid outer boundary condition may also be used. The other boundary condition we use is that, deep into the interior of the disc, the forced solution takes the form of an ingoing wave. This is presumed ultimately to damp through either non-linear or viscous effects. The asymptotic form of the ingoing wave can be found using a WKB approximation such that

$$\xi_r=\frac{\eta\mathrm{e}^{\mathrm{i}\mu}}{\{\Sigma_0 rc[m^2(\Omega-\omega)^2-\Omega^2]^{1/2}\}^{1/2}} \qquad (11)$$

where η is a complex constant and

$$\mu=-\int_r^{r_1}\frac{[m^2(\Omega-\omega)^2-\Omega^2]^{1/2}}{c}\,\mathrm{d}r.$$

Here r_1 is an arbitrary constant radial location chosen such that the WKB approximation is valid inside it.

In addition, we have approximated the rotation to be Keplerian such that $\Omega\equiv\Omega_K$. In the WKB limit the Eulerian velocity perturbations can be found from equation (11) using

$$v_r'=\mathrm{i}m(\Omega-\omega)\,\xi_r,$$

and

$$v_\phi'+\tfrac{1}{2}\Omega\,\xi_r=\frac{-K}{r(\Omega-\omega)}\sim\frac{\mathrm{i}[m^2(\Omega-\omega)^2-\Omega^2]\,\xi_r}{r(\Omega-\omega)(\mathrm{d}\mu/\mathrm{d}r)}.$$

If we use the real parts of the above expressions in equation (7), the flux of negative angular momentum carried by the ingoing waves corresponds to a positive, outward flux:

$$F_H=\pi m|\eta|^2. \qquad (12)$$

Equations (4) and (5) can be combined into a single second-order ordinary differential equation which can be solved by the method of variation of parameters. F_H can be determined from the solution of the unforced equations ($W_2=0$) that satisfies the correct boundary condition (10) (see Papaloizou & Lin 1984). We denote the value ξ_r for this solution by X. At large distances from the companion, this takes on the WKB form

$$X=\frac{C\mathrm{e}^{\mathrm{i}\mu}+C^*\mathrm{e}^{-\mathrm{i}\mu}}{\{\Sigma_0 rc|[m^2(\Omega-\omega)^2-\Omega^2]^{1/2}|\}^{1/2}}$$

where C is a complex constant which satisfies

$$|C|^2=\frac{\Sigma_0 rc^3}{4}\left\{\frac{(\mathrm{d}X/\mathrm{d}r)^2}{|[m^2(\Omega-\omega)^2-\Omega^2]^{1/2}|}+\frac{X^2|[m^2(\Omega-\omega)^2-\Omega^2]^{1/2}|}{c^2}\right\}.$$

We then find that

$$F_H=\frac{\pi}{2|C|^2}\left|\int_R^{r_1}\Sigma_0 rSX\,\mathrm{d}r\right|^2 \qquad (13)$$

where R is the radius of the disc boundary,

$$S=\frac{\mathrm{d}}{\mathrm{d}r}\left(\frac{W_2\beta}{c^2}\right)+\frac{2\Omega\,W_2\beta}{r(\Omega-\omega)c^2},$$

and

$$\beta=\frac{c^2r^2(\Omega-\omega)^2}{c^2-r^2(\Omega-\omega)^2}.$$

This may also be expressed, after an integration by parts, as

$$F_H=\frac{\pi}{2|C|^2}\left|\int_R^{r_1}\frac{\Sigma_0 rW_2Y}{c^2}\,\mathrm{d}r\right|^2. \qquad (14)$$

Here, we have assumed that the effect of the perturbing potential is negligible at large distances from the companion, and Y is equal to the value of K for the unforced solution.

We use the above formalism to calculate the linear response of discs to tidal forcing, and equation (14) to calculate the induced angular momentum transfer between disc and companion for binaries with mass ratios of 1 and 0.1. It is well-known that tidally excited undamped waves have a conserved angular momentum flux or wave action (see, for example, Goldreich & Tremaine 1978; Shu 1984 in the context of planetary rings). Reduction of the wavelength or a decrease in the background density as the waves propagate inwards can then cause them to become non-linear. In the situation considered here, however, the waves are already non-linear when they are launched, and dissipation acts straight away to reduce the wave action as they propagate inwards until low amplitudes are reached. For planetary rings, this phenomenon is documented observationally (see Cuzzi et al. 1984) and theoretically (see Shu 1984). As the wave action decreases, angular momentum is removed from the disc material, causing an accretion flow.

The linear theory is strictly valid for weak forcing as would occur for small discs. For the strong forcing of a gaseous disc considered here, wave amplitudes are likely to be smaller than those predicted by linear theory, because of shock-wave dissipation. As these waves propagate inwards, amplitude decay may cause them to become weak shocks taking the form of a *small*-amplitude wave with a saw-tooth profile (Landau & Lifshitz 1957) propagating with the sound speed. For a barotropic equation of state $P\propto\Sigma^\gamma$, the rate of energy dissipation from a tightly wound weak shock is

$$\Delta\epsilon=\frac{\pi}{6}(\gamma+1)\,r\Sigma_0(\Delta u)^3,$$

where Δu is the velocity difference across the shock. The associated angular momentum loss rate per unit length from the disc is obtained by dividing this by the product of the wavelength of the linear $m=2$ wave and $(\Omega-\omega)$, and is thus approximately $m\Delta\epsilon/(2\pi c)$. This angular momentum transport must cause F_H to decrease into the disc (see Papaloizou & Lin 1984) such that

$$\frac{\mathrm{d}F_H}{\mathrm{d}r}=\frac{m}{12c}(\gamma+1)\,r\Sigma_0(\Delta u)^3.$$

From equations (12) and (11), using the large m limit which remains reasonably accurate even for $m=2$,

$$F_H = \frac{\pi \Sigma_0 r c (u_A)^2}{4(\Omega - \omega)}.$$

Thus

$$\frac{r}{F_H}\frac{dF_H}{dr} = \frac{m}{3\pi c^2}(\gamma+1)\, r(\Omega-\omega)\frac{(\Delta u)^3}{u_A^2},$$

where u_A is the radial velocity excursion. From the above, we see that the local scalelength on which F_H decreases becomes comparable with the disc radius when $(\Delta u)^3 \sim (c u_A^2)/\mathcal{M}$. This indicates that, for high Mach numbers, the non-linear waves become weak shocks before they have propagated very far into the disc.

If the shock discontinuity is as much as the wave amplitude, $\Delta u \sim u_A$, and the above gives $\Delta u \sim c/\mathcal{M}$ only, with a corresponding dissipation rate per unit length equivalent to that due to a shear viscosity with $\alpha \sim \mathcal{M}^{-3}$, neglecting multiplicative constants of order unity. Larson (1990) finds, however, that shock discontinuities disappear if u_A is below a critical value $u_{Ac} \sim 0.2c$ for $m=2$. In such a case, for high Mach numbers we should use $(\Delta u)^3 \sim (c u_{Ac}^2)/\mathcal{M}$. The corresponding α is then $\sim (u_{Ac}/c)^2 \mathcal{M}^{-1}$. In the large Mach number limit, this form of α is consistent with the expression given by Larson (1990) which is also consistent with the results of Spruit (1987). But note that, if there is a critical amplitude, shock dissipation may not continue even at this level as the waves propagate inwards, if for example, there is a surface density increase which could cause the waves to reduce their amplitude below the critical value.

4 NON-LINEAR NUMERICAL SOLUTIONS

4.1 Numerical methods

We present here numerical results obtained with two numerical methods. The first is a two-dimensional explicit finite difference scheme on an equally spaced Eulerian grid in cylindrical coordinates, which uses the flux-vector splitting method of van Leer (1982) to calculate the fluxes used in the conservation-law form of the equations. The ADI method of Beam & Warming (1978) is used to advance the equations in time. It is based on a multidimensional, Second-order Alternating Direction Implicit/Explicit hydro-code, or SADIE for short, developed by Arnold (1985). This method was applied by Heemskerk, Papaloizou & Savonije (1992) to self-gravitating discs. There is no need for artificial viscosity terms to be added to the equations, shocks being handled by the internal differencing. This method solves the equations for an ideal gas with specific heat ratio $\gamma = 5/3$ in conservation-law form. The model is strictly two-dimensional, producing the barotropic equation of state with $P = \text{constant} \times \Sigma^\gamma$, by including the required amount of local cooling in the energy equation. This is needed because when shocks are present they act to increase the local entropy.

We use an equally spaced grid in cylindrical coordinates, with 200 zones in the radial direction and 64 zones in the azimuthal direction, to integrate the set of equations given above but with no viscosity. We work in a frame corotating with the binary, with the centrifugal and Coriolis forces included as source terms in the conservation laws. Owing to the explicit nature of the difference scheme, the maximum time-step Δt we can take to integrate the numerical equations is limited by the well-known Courant–Friedrich–Lewy condition. In our simulations we took $\Delta t = 0.70 \Delta t_{\rm CFL}$.

We remark that care needs to be taken in using this code for non-self-gravitating discs. Angular momentum was found to diffuse radially due to code truncation errors. This effect is significant for surface density profiles with relatively large gradients in them, independent of whether shocks were present. This effect could result in an $m=0$ diffusive instability which produces ring-like features in the surface density and angular momentum profiles over long time-scales. In our calculations we rewrote the ϕ-component of the equation of motion as a conservation law in terms of $r^{1/2}\Sigma v_\phi$. By adopting a constant initial surface density Σ_0, this quantity is initially constant (Keplerian rotation). In this way such instabilities were avoided over the run times of our calculations.

In order to investigate the effects of viscosity on the tidal response, we solved the equations, including additional viscosity terms in the equations of motion (1) and (2), using a second method. This solves the equations by explicit finite difference techniques using operator splitting. The advection terms are handled using van Leer's monotonic transport scheme (see, for example, Kley 1989). We used a strictly polytropic equation of state and note that, for inviscid discs, methods 1 and 2 yielded very similar characteristics for the propagating waves induced by tidal effects over the times for which our computations were run.

4.2 Numerical results

We now present the results of non-linear calculations of the forced response to tidal perturbations of discs in binary systems with mass ratios of 1.0 and 0.1 (see Table 1). The calculations with SADIE were performed for discs with varying initial size and Mach number $\mathcal{M}_0$. This is here defined as the ratio of orbital speed to sound speed at the disc inner boundary, where $r = r_0$, which was treated as rigid. The initial surface density profile was taken to be uniform and equal to Σ_0 for $r_0 < r < r_1$, where r_1 corresponds to the outer boundary.

Note that, because we have a simple equation of state, $P \propto \Sigma^\gamma$, knowledge of the initial Mach number at the inner boundary enables this quantity to be calculated elsewhere at other times. If we use $c \propto \Sigma^{(\gamma-1)/2}$, and the approximate validity of Kepler's law, we obtain

$$\mathcal{M} = \mathcal{M}_0 (\Sigma_0/\Sigma)^{(\gamma-1)/2} (r_0/r)^{1/2}.$$

In each case the unit of mass and the unit of length were chosen such that the total binary mass and the binary separation were unity. The unit of time is then defined by adopting unity for the gravitational constant, so that one orbital period corresponds to 2π time units. Because the disc is non-self-gravitating, the results are independent of the magnitude of the initial surface density, so any value for this may be taken. For convenience we shall adopt a value such that the total disc mass is unity. Note that the numerical values for tidal torque given below scale in proportion to the disc mass. In

Table 1. The various inviscid model calculations. $\mathcal{M}_0$ is the initial Mach number of the Keplerian rotation at the disc's inner boundary r_0, r_1 is the outer disc radius, Σ_0 is the initial constant surface density in the disc, q is the mass ratio, whereby the (primary) companion with the disc is the most massive, and $\mathcal{T}^{\text{lin}}$ and $\mathcal{T}^{\text{nonlin}}$ are the total tidal torques between the companion star and the disc obtained from the linear and non-linear numerical calculations, respectively. In our units the binary separation is unity.

Model	$\mathcal{M}_0$	q	Σ_0	r_0	r_1	$\mathcal{T}^{lin}$	$\mathcal{T}^{nonlin}$
1	10	1	2.37	0.095	0.379	7.3×10^{-3}	1.8×10^{-3}
2	25	1	4.20	0.071	0.284	7.8×10^{-4}	2.4×10^{-4}
3	50	1	4.20	0.071	0.284	4.5×10^{-4}	1.4×10^{-4}
4	10	0.1	1.02	0.145	0.578		
5	50	0.1	1.02	0.145	0.578	2.6×10^{-3}	6.0×10^{-4}

each case the calculation is continued until a quasi-steady state response is attained. This is achieved even though the only dissipation that occurs is that due to shocks. The tidal forcing induces a trailing spiral pattern with an associated outward angular momentum flow which is ultimately communicated to the companion via a tidal torque. As expected, effective open spirals are associated with large discs and low Mach numbers. The ratio of outer boundary radius to inner boundary radius is characteristically about four in these calculations. This has been chosen for convenience and is small compared to that expected for most examples of astrophysical discs. However, we are primarily interested in calculating the response to tidal forcing and this range of radii is probably reasonable for this purpose.

Model 1. This model is designed to illustrate that the local angular momentum balance in the disc is determined by the net result of wave transport of angular momentum and local gravitational interaction with the companion star via a tidal torque which can act as a source or sink of disc angular momentum. To do so, we adopt, in model 1, a unit mass ratio and a low initial Mach number (~ 10), and the disc's outer boundary equals the (spherical) Roche radius. In Fig. 1 we show the surface density, which exhibits a strong two-armed spiral at a time of 20.3 units (about three binary orbital periods), at which time the form has become quasi-steady. The tidally induced radial velocity perturbations in the disc are less than 60 per cent of the sound speed, except for the outer regions of the disc ($r \geq 0.27$) where supersonic values are attained. In these outer regions, shock dissipation gives rise to effective absorption of angular momentum by the companion star, which causes the matter to fall inwards. In this way the region between the two outer spiral arms is effectively cleared of matter. In Fig. 2 we show the azimuthally averaged advected angular momentum flow rate and the azimuthally averaged external applied tidal torque density, i.e. the azimuthally averaged external torque per unit surface in the disc as a function of radius. The positive (outward) wave transport of angular momentum associated with the induced trailing spiral wave allows mass to move inwards and produces the centrally concentrated (azimuthally averaged) surface density profile shown in Fig. 3. The external torque density alternates in sign, being negative in the regions with $r \leq 0.18$ and $r \geq 0.27$, and positive in the region in between. The strong decline of the angular momentum flow for $r \geq 0.27$ in Fig. 2 is caused by shock dissipation and associated angular momentum transfer to the companion star via the tidal torque. The residual, integrated, tidal torque is 2×10^{-3}, allowing accretion on a time-scale of about a thousand binary orbits. For comparison, the total angular momentum transfer rate to the companion, calculated from the linear response of the initial model as described above, using equation (14), was 7.3×10^{-3}. This value is a factor of four larger than that found from the non-linear numerical calculations. We regard this difference, however, as being explicable by the fact that the surface density in the non-linear calculations becomes significantly depressed relative to the initial model at large radii (see Fig. 3). We also calculated a model with the same parameters but with a smaller outer disc radius of 75 per cent of the spherical Roche radius. The quasi-steady state, and the angular momentum transfer rate to the companion were in good agreement with those found in the model described above.

Model 2. This model is constructed to illustrate that the above favourable result for tidally driven accretion is strongly dependent on having a low Mach number and a large disc almost filling its Roche lobe. In model 2, we choose an initial Mach number of 25, and an outer disc radius 75 per cent of that in model 1. The quasi-steady surface density for model 2 is shown after a time 22.96 in Fig. 4. Spiral waves are excited but in the form of a more tightly wound spiral than model 1. The tidally induced radial velocity perturbations in the disc attain supersonic values for $r \geq 0.24$, i.e. in the outermost spiral arm. The region between the spiral arms is effectively cleared of matter in this outer part of the disc. Fig. 5 shows the azimuthally averaged angular momentum flow rate and the azimuthally averaged external torque density as a function of radius. The steep decay of the angular momentum flux for $r \geq 0.25$ is again caused by shock dissipation and associated transfer of angular momentum to the companion star via the tidal torque in the outermost regions of the disc. The external torque density alternates in sign in conjunction with the spiral density wave in the disc, whereby its amplitude slowly increases with radius, as expected. Because of the short wavelength of the response and the long length-scale of the exciting tidal force, cancellation leads to a small residual integrated tidal torque $\mathcal{T} = 2.4\times10^{-4}$, which is almost an order of magnitude less than for model 1. The value 7.8×10^{-4} for the torque follows from the linear theory applied to the initial model. In this case the surface density in the outer parts suffers much less depression relative to the initial model as a result of the less effective tidal interaction. It can be seen in Fig. 4 that the waves decay with decreasing radius. The fact that the waves can still decay, even though they have small amplitude as they propagate inwards, is because they appear to develop a saw-tooth form corresponding to weak shocks. This can provide residual dissipation at low amplitudes (Landau & Lifshitz 1957).

Model 3. The situation is even more extreme for model 3, which was identical to model 2, but with a higher initial Mach number of 50. The surface density at time 14.06 is shown in Fig. 6. The spiral form is very tightly wrapped and decays before the inner boundary is reached. The spiral wave extends further inward than is shown in the grey-scale plot, as can be seen in Fig. 7, which shows the azimuthally averaged angular momentum flux and external torque density through the disc. Note that the external torque density in the outer

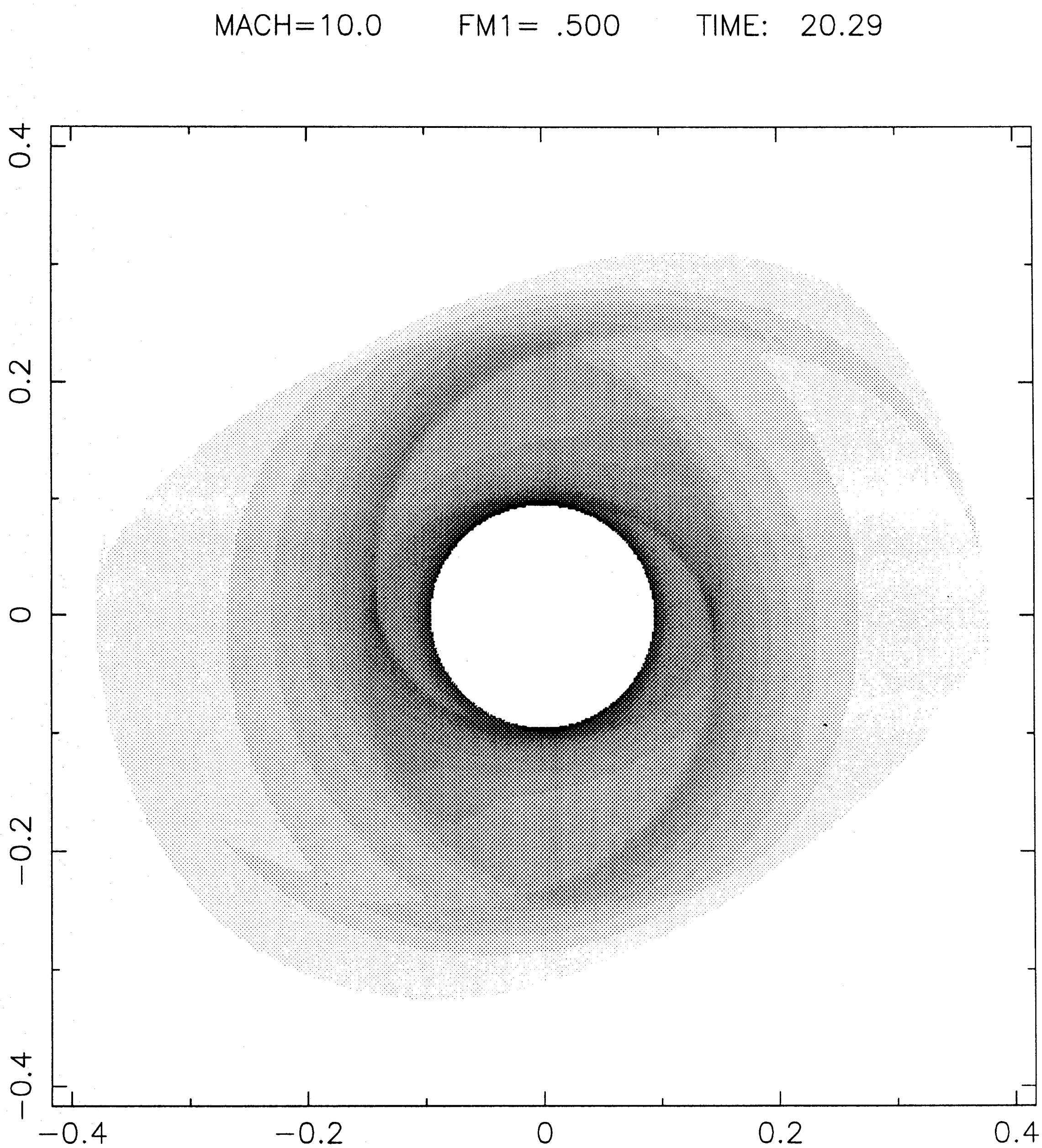

Figure 1. Grey-scale plot of surface density distribution in the disc for model 1 at time 20.3.

parts of the disc is an order of magnitude larger than for model 2. Cancellation effects caused by the rapidly alternating external torque density are strong, however, so that the residual tidal torque is rather weak at 1.4×10^{-4}, somewhat smaller than the linear value $F_H = 4.5 \times 10^{-4}$. The waves are unable to affect the azimuthally averaged surface density profile in the inner region of the disc, which is still uniform (see Fig. 8). For this high Mach number case, supersonic radial velocity perturbations are induced for $r \geq 0.19$. Hence strong dissipation occurs in a more extended region than in models 1 and 2, which contributes to the decay of the spiral pattern in the inner regions of the disc.

It may seem paradoxical that, in the quasi-steady state, the net tidal torque is stronger in model 1 than in models 2 and 3, even though there is less matter in the outer parts of the disc in model 1. We believe, however, that this is a consequence of the different Mach numbers in the outer regions of the disc in these cases. At a radius of 0.27, this was round 6.8 in model 1, 16 in model 2, and 28 in model 3. Although we should not expect a complete explanation from linear theory, this none the less shows that, other things being equal, a lower Mach number gives a deeper response to the tide and a stronger torque, which approximately scales inversely with Mach number (Table 1). This comes about from the be-

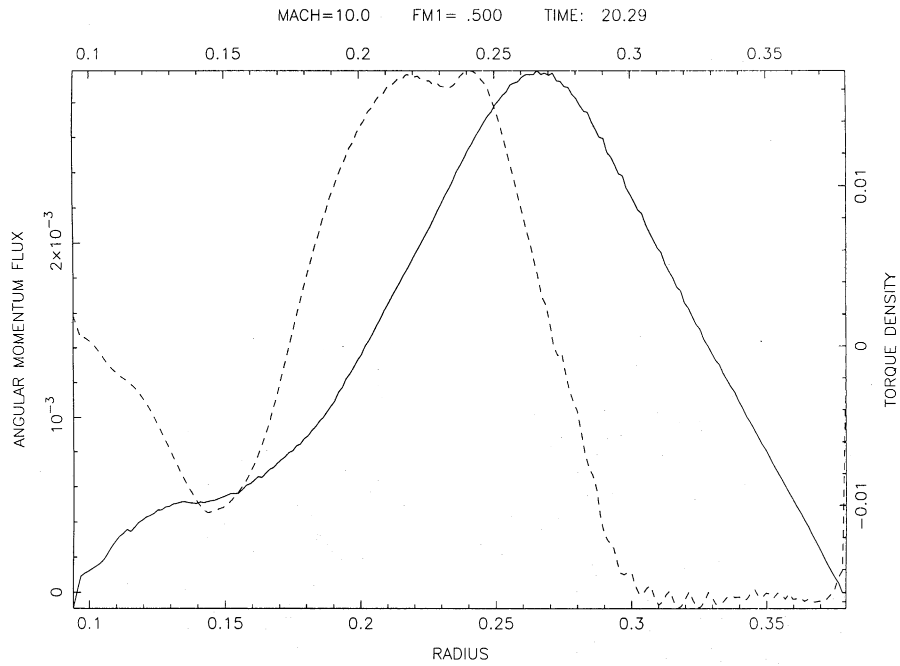

Figure 2. The azimuthally averaged advected angular momentum flux (full line) and tidal torque density (dotted line) as a function of radius for model 1 at time 20.3.

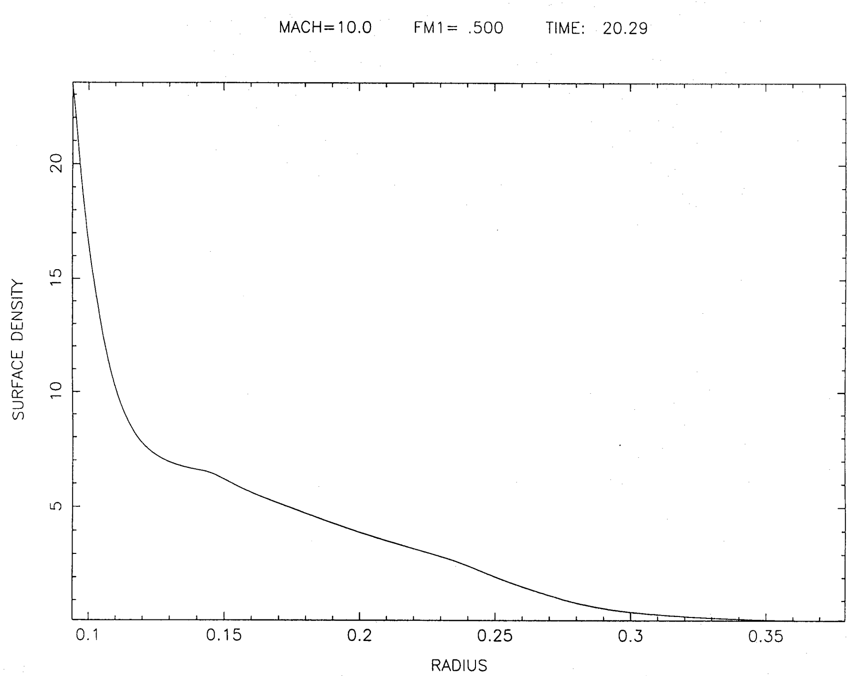

Figure 3. The azimuthally averaged surface density in the disc as a function of radius for model 1 at time 20.3.

haviour of the integral in equation (13), which determines the tidal torque. The integrand here involves a free perturbation solution X which alternates in sign as it represents a sound wave. The result of this is that the integral tends to zero as the wavelength, which is proportional to $1/\mathscr{M}$, does. Normally one expects that the integral tends to zero as $1/\mathscr{M}$ (but it could be faster) and then, from equation (13), the torque also tends to zero in this manner.

This result indicates that, other things being equal, there should be a lower surface density in the outer regions of the initially low Mach number discs compared to those with higher Mach number, as is seen in the calculations. It is also

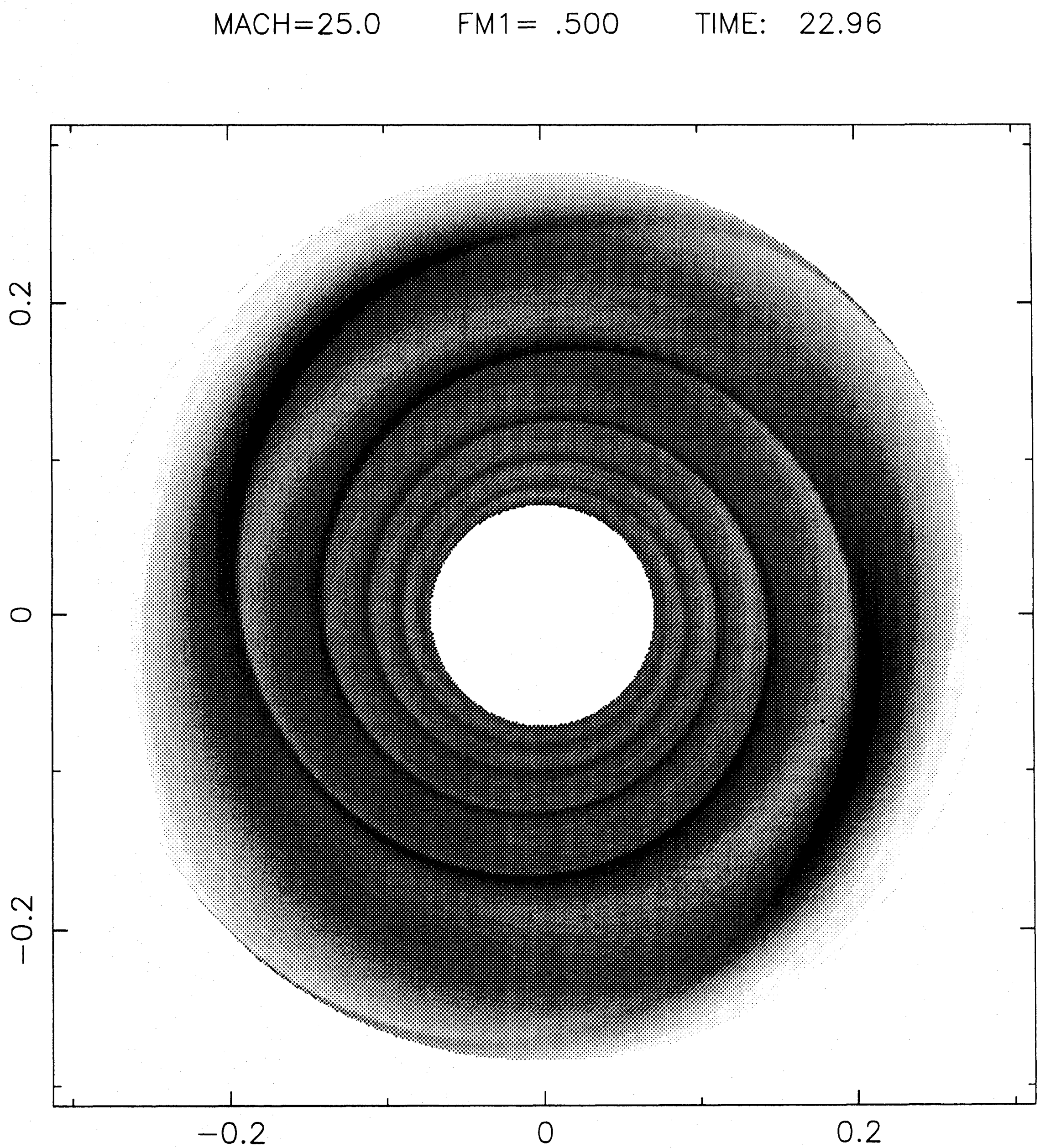

Figure 4. Grey-scale plot of surface density distribution in the disc for model 2 at time 22.96.

worth noting that the product of the wavenumber and the local radius of the excited wave is characteristically equal to $\mathscr{M}$. Thus for model 1, the distance between the outer part of the disc and the simply (Keplerian) calculated location of the 2:1 resonance, which is at $r = 0.5$, is about one wavelength. Although the resonance is not in the disc and orbits would be very strongly perturbed at its location, the increase in the number of wavelengths between this location and the disc edge as the Mach number increases also fits in with the expectation that the torque will be weaker in the higher Mach number cases.

Model 4. We also performed calculations (models 4 and 5) for a companion mass of 0.1. In this case, because the 2:1 inner Lindblad resonance, simply calculated to be at $r = 0.61$, can approach the disc outer boundary, two-armed spiral waves are more readily excited.

For model 4, with $\mathscr{M}_0 = 10$, the calculation was similar to model 1 in that it produced a strong two-armed spiral response in the surface density, which is plotted in Fig. 9. The azimuthally averaged surface density profile rapidly became peaked at the inner boundary as in model 1, indicating very strong tidal effects. The tidal torque in fact decreased to very small values as most matter was cleared from the outer part of the disc for $r > 0.4$ (the region of shock dissipation) and no meaningful comparison could be made with linear theory.

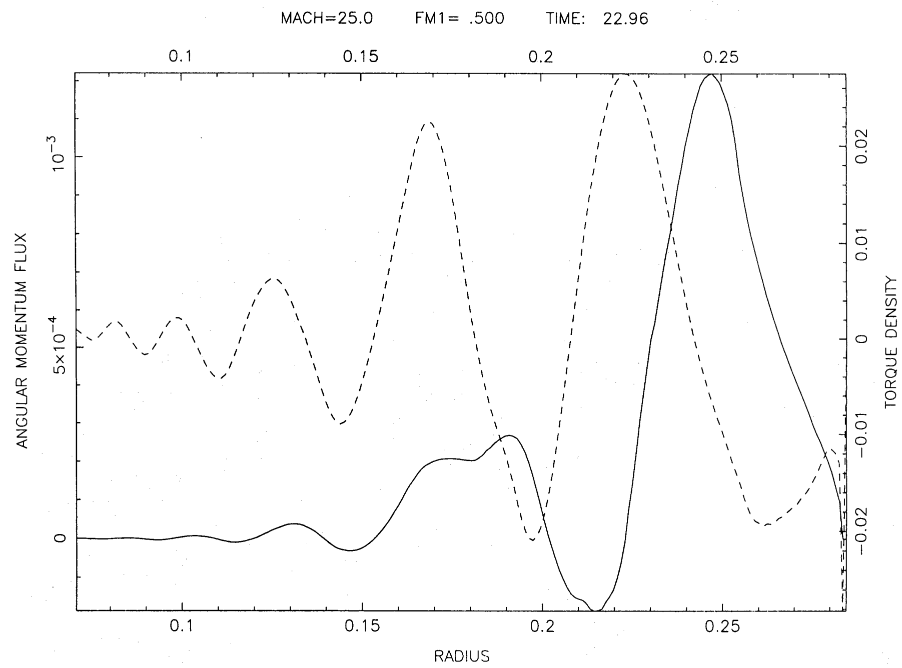

Figure 5. The azimuthally averaged advected angular momentum flux (solid line) and tidal torque density (dashed line) as a function of radius for model 2 at time 22.96.

Model 5. The response, however, is much weaker in model 5, which was the same as model 4, but with an initial Mach number, $\mathscr{M}_0$, of 50. The surface density is shown in Fig. 10. The spiral form is more tightly wound and decays before the inner boundary is reached. Supersonic radial velocities occur for $r \geq 0.3$. The tidal torque is quite strong (6×10^{-4}) compared to 2.6×10^{-3} calculated for the initial model using linear theory. The difference may be due to the fact that, although the surface density profile in the inner regions is unaffected for $r < 0.3$, the tidal torque produced a pronounced azimuthally averaged surface density maximum of about 2.5 times the initial value at $r = 0.42$ owing to the infall of matter from the disc's outer region (Fig. 11).

In this context we remark that the linear torques were computed with a uniform surface density profile and a rigid outer boundary condition, as in the initial models. This is naturally expected to give an overestimate for the final torques. We comment that linear calculations with smaller outer boundary radii or tapering surface density profiles give significantly lower torques.

4.3 The effect of shear viscosity

In order to examine the effects of viscosity on these calculations, we performed calculations for discs with varying amounts of shear and radial viscosity using method 2. According to linear theory, the presence of these viscosities is expected to cause the sound waves excited by the tidal effect to be damped (see Lin & Papaloizou 1993 and references therein). In addition, a non-zero shear velocity causes the disc to expand which induces an increase in the tidal forcing. Here we use the usual alpha prescription for the viscosity, i.e. $\nu\Sigma = \frac{2}{3}\alpha P \Omega^{-1}$, with a corresponding α_r appropriate to the viscosity coefficient ν_r. To demonstrate the reduction of wave amplitude that occurs when internal viscosities are introduced, we studied model 6 using method 2, which approximately corresponds to model 2 with a mass ratio of unity except that $r_0 = 0.1$ and $r_1 = 0.3$. The initial Mach number at the inner boundary, for purposes of comparison with model 2, was 31. For this model, we adopt $\alpha = 0.01$ and $\alpha_r = 0$. In Fig. 12 we show the quasi-steady state surface density plot. This shows a similar pattern of wave excitation to that in model 2 except that the wavelengths are slightly shorter because of the somewhat smaller sound speed. As expected, the waves are relatively undamped in this case. Additional calculations with a smaller value of r_0 showed that the waves did not propagate significantly further in than $r = 0.1$. We found that our results were sensitive to internal viscosity parameters; in particular, wave amplitudes were sensitive to the magnitude of α_r as well as to the Mach number. In Fig. 13 we show the quasi-steady state surface density plot for model 7 which had identical parameters to model 6 except that $r_0 = 0.05$, $\alpha = 0.1$ and $\alpha_r = 0.4$. In this case the disc fails to truncate before the outer boundary radius and wave excitation is almost completely eliminated. In this series of calculations we found that for discs in which the Mach number was three times higher, waveforms could only be produced very close to the outer boundary. These results, and the lack of truncation of the above model, are consistent with results given in Lin & Papaloizou (1993), who used a scheme with a non-zero α_r.

5 DISCUSSION

We have considered time-dependent non-linear hydrodynamic calculations of accretion discs in close binary systems with mass ratios of unity and 0.1. We have considered a range of disc sizes, Mach numbers and disc viscosities with the aim of studying the excitation of waves by tidal inter-

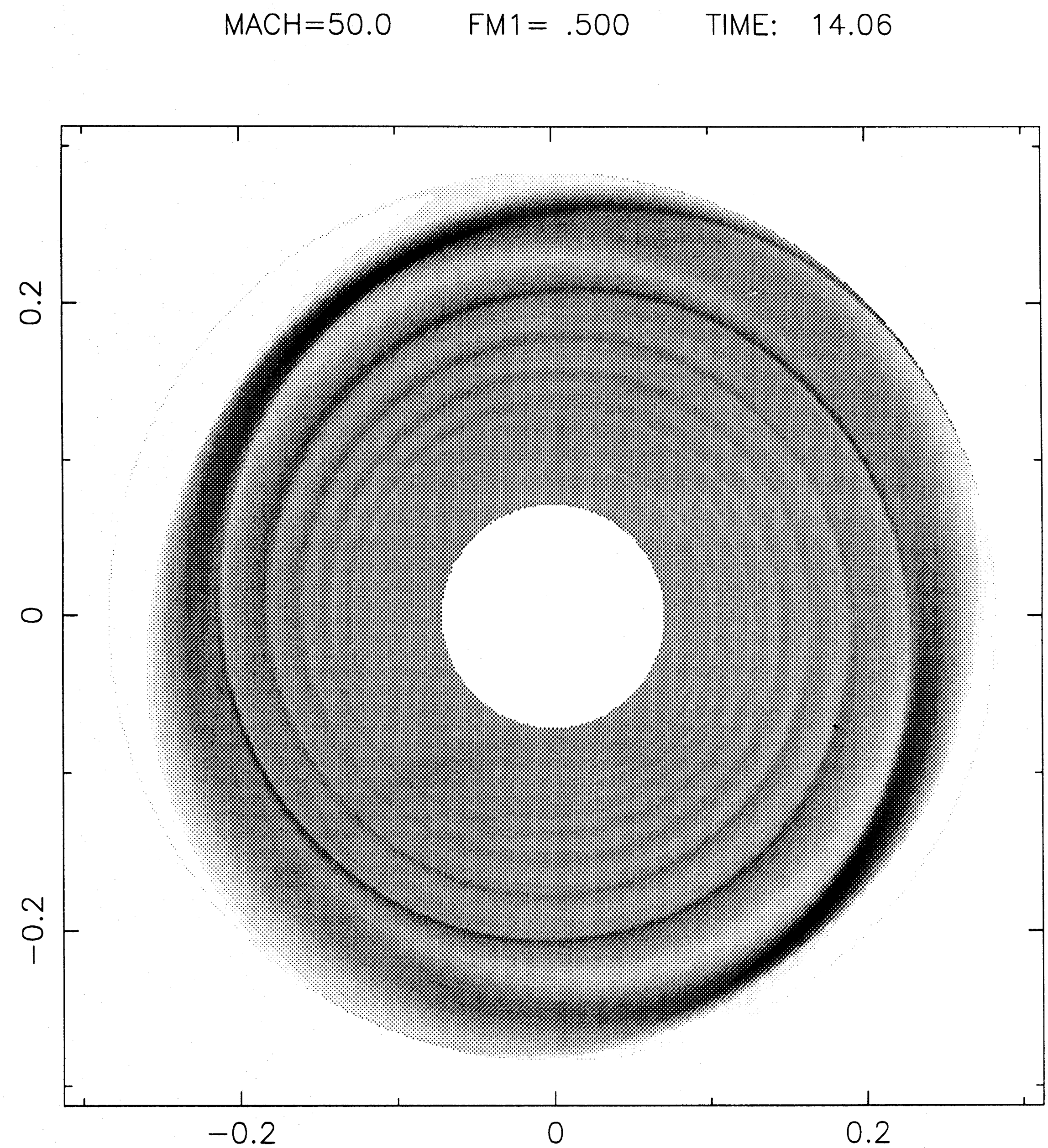

Figure 6. Grey-scale plot of surface density distribution in the disc for model 3 at time 14.1.

action. We verify wave excitation and the existence of an $m=2$ spiral response for both mass ratios considered. Wave excitation occurs, although the centre of the inner Lindblad resonance lies outside the disc because the resonance has a finite width and can be thought of as still partially overlapping the disc. The angular momentum fluxes generated in the calculations are consistent with those predicted by linear response calculations.

We find, in agreement with previous work (Sawada et al. 1987; Spruit et al. 1987; Różyczka & Spruit 1989; Matsuda et al. 1989; Spruit 1989), that extensive low Mach number (<10) discs, which almost fill the Roche lobe, have significant waves in them that can propagate to small disc radii and transfer angular momentum outwards even when the only dissipation that occurs is due to shocks. For internal Mach numbers greater than about 25, however, as might have been expected from the scaling of their effective α with Mach number given by Spruit (1987), the waves are much weakened and fail to propagate with significant amplitude very far into the disc and so hardly affect the surface density profile except at large radii. The best that could be expected in such cases is that significant waves could reach small radii if the surface density decreases rapidly inwards. The effect would be significantly reduced, however, if the outer regions of the disc were absent, as might eventually result on account of tidal interaction over long time-scales. Thus our calculations indicate that wave-driven accretion is unlikely to be able to proceed rapidly enough through discs with modest outer

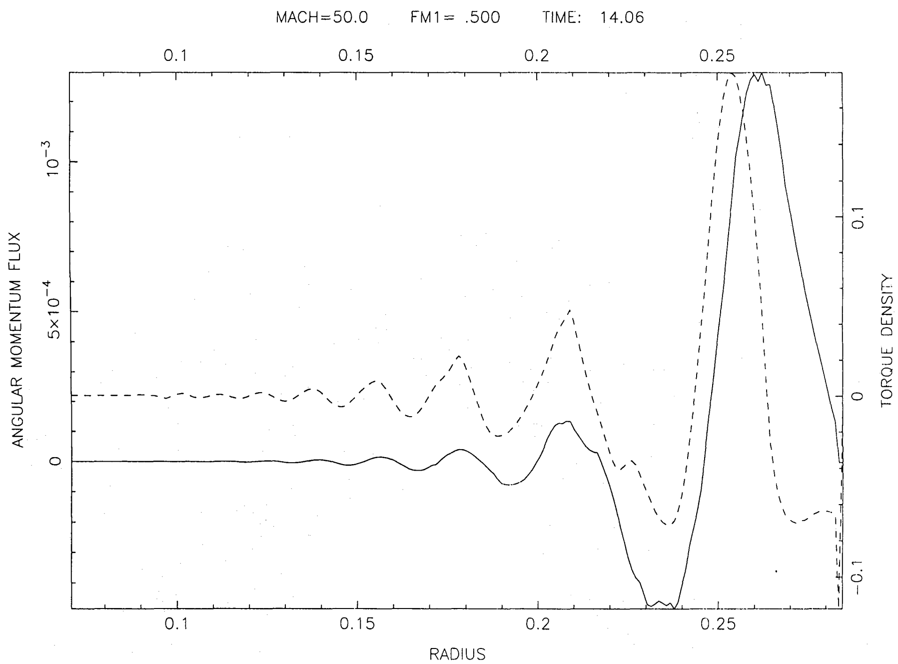

Figure 7. The azimuthally averaged advected angular momentum flux (solid line) and tidal torque density (dashed line) as a function of radius for model 3 at time 14.1.

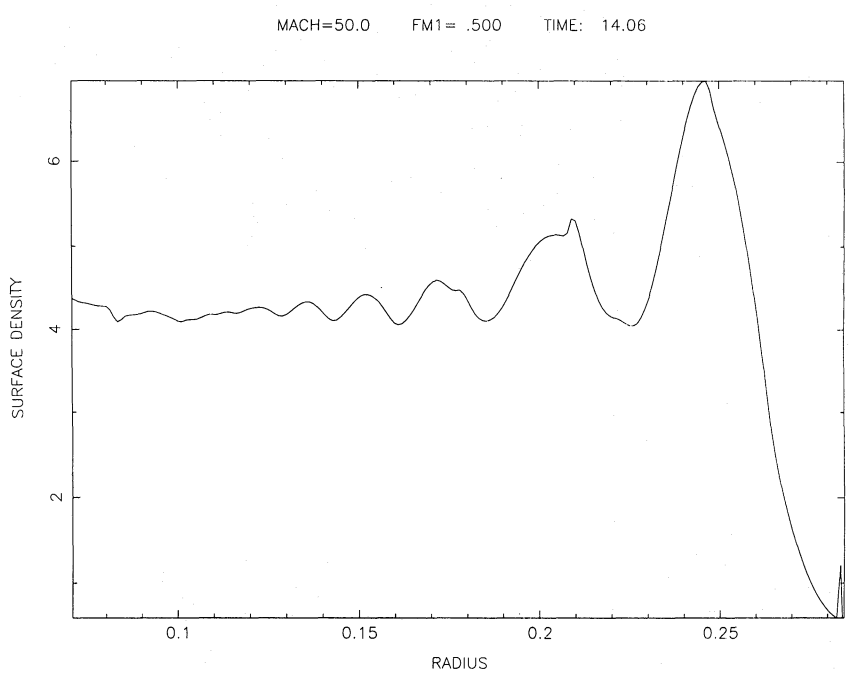

Figure 8. The azimuthally averaged surface density in the disc as a function of radius for model 3 at time 14.1.

radii and Mach numbers ≥ 25. This is also fully consistent with the discussion at the end of Section 3.

In particular, although an adequate tidal torque for disc truncation may be produced, excited waves are likely to be too weak to play an effective role in causing accretion through observed discs in such objects as cataclysmic variables, in which observations require, under outburst conditions, a viscosity parameter α of about 0.1 (Pringle

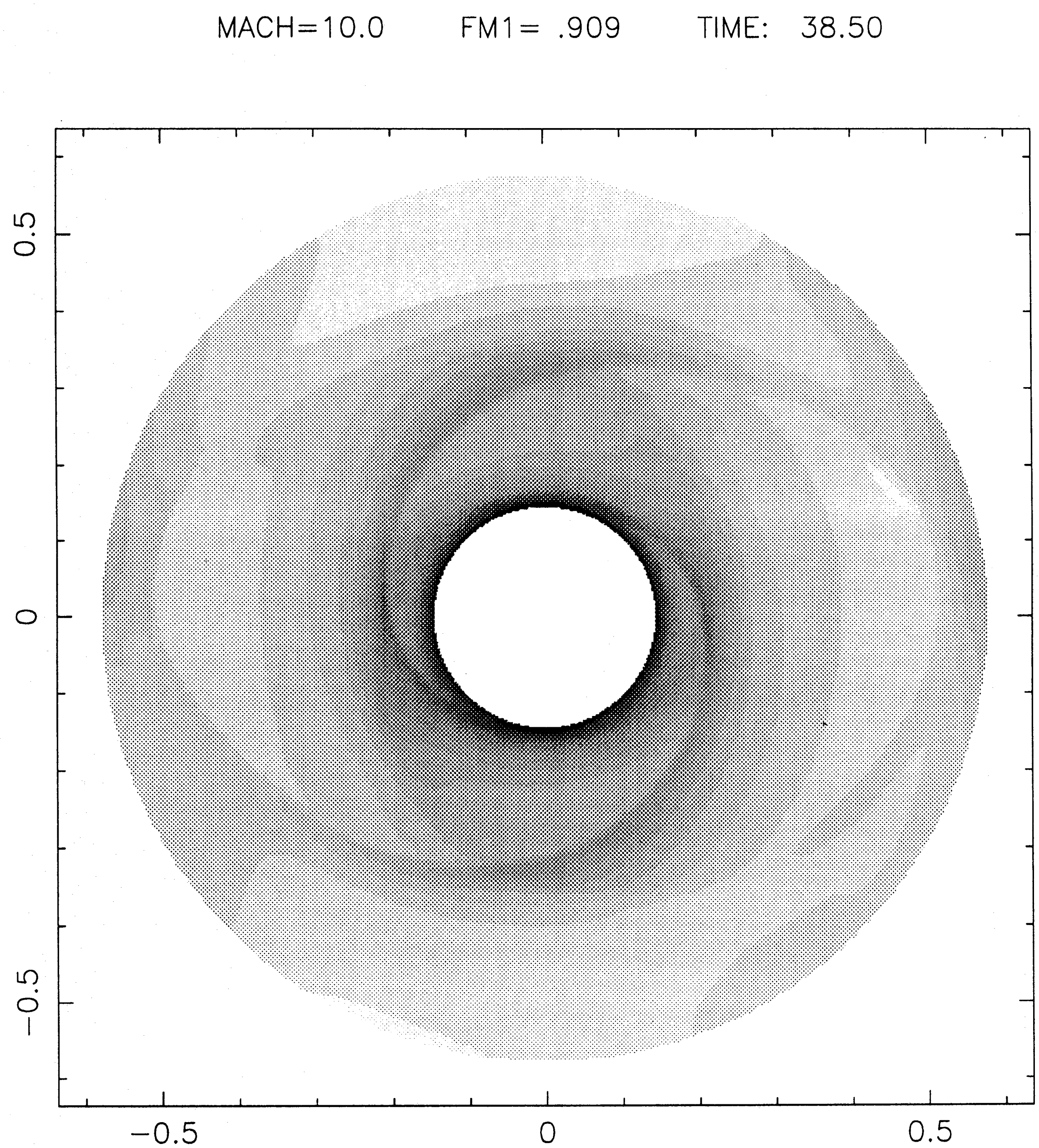

Figure 9. Grey-scale plot of surface density distribution in the disc for model 4 at time 38.5.

1981) as well as Mach number ≥ 25. In addition, we found that the waves are damped by internal viscosities corresponding to the appropriate α parameters exceeding this value. The presence of strong absorption lines indicates that the disc is opaque to continuum radiation during the outbursts (Mayo, Wickramasinghe & Whelan 1980) so that the disc may be thermally stratified. In this case, three-dimensional effects, such as the upward tilting of inward-propagating wave fronts due to the vertical variation of sound speed with height, might be important (Lin et al. 1990a,b). During the quiescence, the strong Balmer emission lines indicate that the disc is optically thin and therefore it is likely to have an essentially isothermal vertical structure (Williams 1980). Although refraction is no longer effective in this limit, the above results suggest that tidally induced waves are unlikely to propagate far into the disc since both the continuum (Wood et al. 1989) and line spectrum (Williams & Ferguson 1982) indicate a low ($<10^4$ K) temperature throughout the disc (Lin, Williams & Stover 1988) such that the corresponding Mach number is larger than 50. Thus we expect the tidal response of the disc to be for the most part weak, being such that most of the tidal torque induced by the

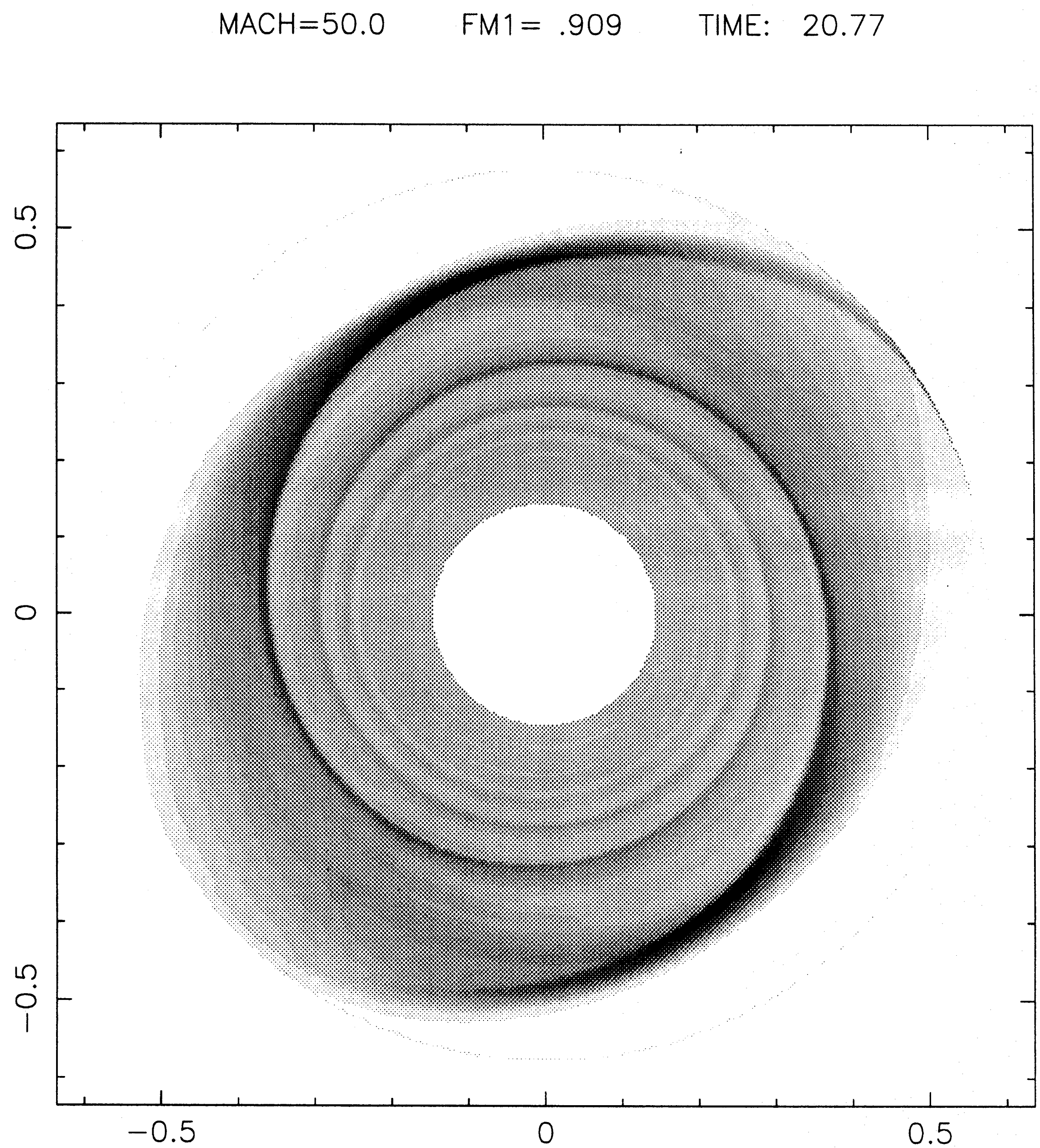

Figure 10. Grey-scale plot of surface density distribution in the disc for model 5 at time 20.77.

companion arises in the outer regions of the disc. Detailed models of the emission-line profile of SS Cyg suggest that the efficiency of non-linear dissipation increases with the disc radius such that most of the radiation is emitted in the outermost region of the disc where the tidal disturbance is dominant (Cheng & Lin 1992). This radial dependence in the dissipation pattern is consistent with the above consideration.

Although tidally induced density waves may not be the dominant carrier of mass and angular momentum throughout discs in cataclysmic variables, they are more likely to play an important role in protostellar discs around T Tauri binary stars. In typical protostellar discs, the Mach number is relatively small (~ 10) (Lin & Papaloizou 1985). Thus we might expect a strong internal disc response to the tidal forcing of the binary. In one particular T Tauri binary star, GW Ori, both circumstellar (interior to the binary orbit) and circumbinary (exterior to the binary orbit) discs have been inferred from infrared excesses in the continuum radiation (Mathieu, Adams & Latham 1991). Quantitatively, these

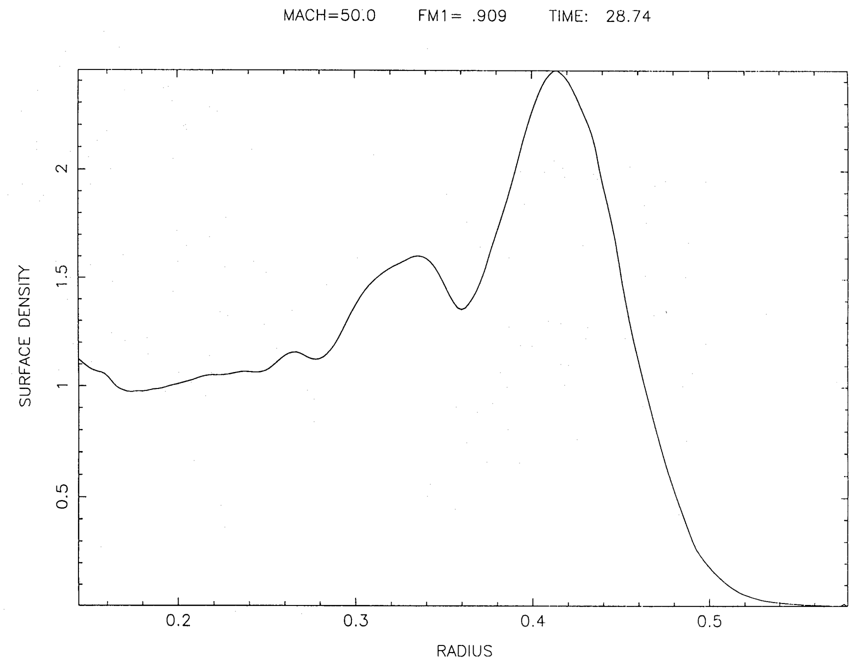

Figure 11. The azimuthally averaged surface density in the disc as a function of radius for model 5 at time 28.74.

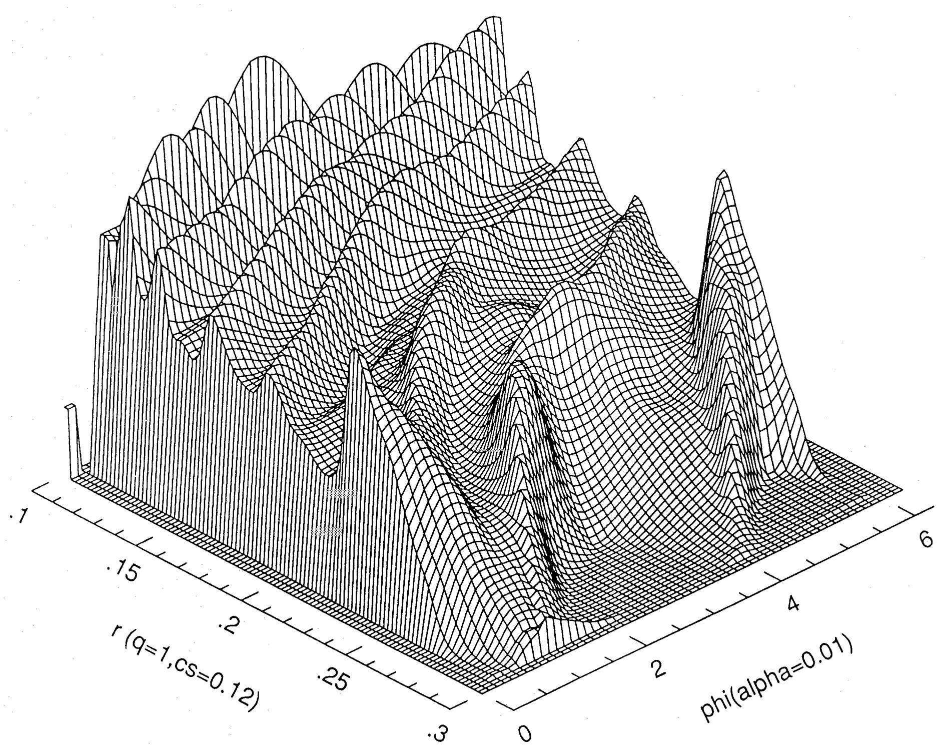

Figure 12. The quasi-steady state surface density in the disc as a function of radius and azimuth for model 6.

data suggest that the circumstellar disc may have a Mach number of order 10. In this case, we anticipate that the disc response to the tidal disturbance might be significant. With typical values for the surface density, the excess infrared luminosity may be entirely attributed to the dissipation of the density waves excited by the binary's tidal torque. Simple estimates suggest, however, that such energy dissipation and angular momentum transfer could lead to a rapid depletion of the circumstellar disc if it is tidally truncated. The long-term preservation of any observable signatures of discs around T Tauri binary stars requires further investigation and will be discussed elsewhere.

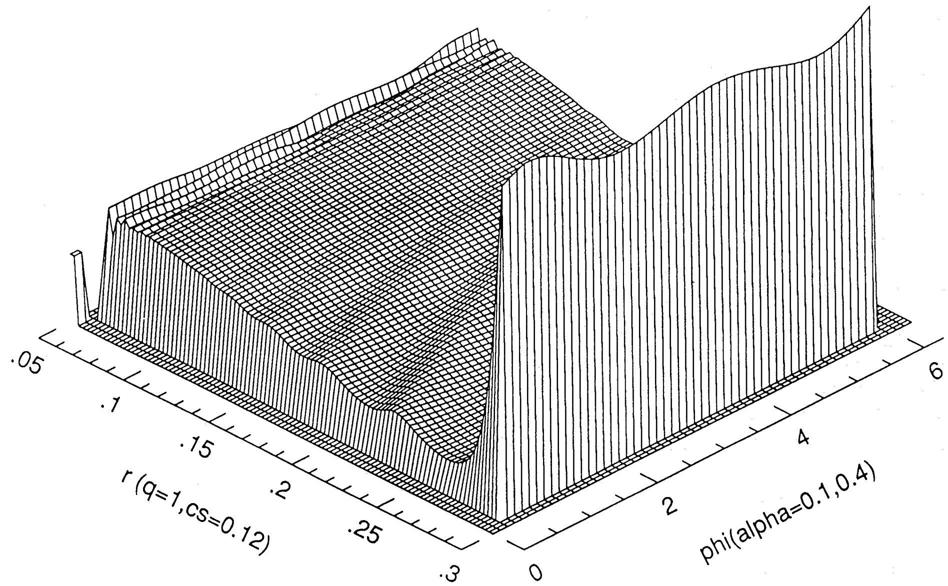

Figure 13. The quasi-steady state surface density in the disc as a function of radius and azimuth for model 7.

ACKNOWLEDGMENTS

We thank Dr H. Spruit for useful conversation. JCBP thanks CHEAF; GJS and DNCL are grateful to QMW for hospitality. This work was supported in part by NASA grant NAGW 2422 and the SERC QMW rolling theory grant (GR/H/09454).

REFERENCES

Arnold C. N., 1985, PhD thesis, Univ. Microfilms, Ann Arbor, Michigan, USA
Beam R. M., Warming R. F., 1978, AIAA, 16, No. 4, 393
Cheng F. H., Lin D. N. C., 1992, ApJ, 389, 714
Cuzzi J. N., Lissauer J. J., Esposito L. W., Holberg J. B., Marouf E. A., Tyler G. L., Boischot A., 1984, in Greenberg R., Brahic A., eds, Planetary Rings. Univ. Arizona Press, Tucson, p. 73
Donner K. J., 1979, PhD thesis, Univ. Cambridge
Goldreich P., Tremaine S., 1978, Icarus, 34, 240
Goldreich P., Tremaine S., 1980, ApJ, 241, 425
Heemskerk M. H. M., Papaloizou J. C. B., Savonije G. J., 1992, A&A, 260, 161
Kley W., 1989, A&A, 222, 141
Landau L., Lifshitz E., 1957, Hydrodynamics, Pergamon Press, Oxford
Larson R. B., 1990, MNRAS, 243, 358
Lin D. N. C., Papaloizou J. C. B., 1985, in Black C. D., Matthews M. S., eds, Protostars and Planets II. Univ. Arizona Press, Tucson, p. 981
Lin D. N. C., Papaloizou J. C. B., 1986, ApJ, 307, 395
Lin D. N. C., Papaloizou J. C. B., 1993, in Levy E., Lunine J., Matthews M. S., eds, Protostars and Protoplanets III. Univ. Arizona Press, Tucson, in press
Lin D. N. C., Pringle J. E., 1976, in Eggleton P. P., Mitton S., Whelan J. A. J., eds, Proc. IAU Symp. 73, Structure and Evolution of Close Binary Stars. Reidel, Dordrecht, p. 237
Lin D. N. C., Papaloizou J. C. B., Savonije G. J., 1990a, ApJ, 364, 326
Lin D. N. C., Papaloizou J. C. B., Savonije G. J., 1990b, ApJ, 365, 748
Lin D. N. C., Williams R. E., Stover R. J., 1988, ApJ, 327, 234
Lubow S., Shu F. H., 1975, ApJ, 198, 383
Lynden-Bell D., Pringle J. E., 1974, MNRAS, 168, 603
Mathieu R. D., 1992, in Kondo Y., Sistero, Polidan R., eds, Proc. IAU Symp. 151, Interacting Binary Stars. Reidel, Dordrecht, p. 21
Mathieu R. D., Adams F. C., Latham D. W., 1991, AJ, 101, 2184
Matsuda T., Inoue M., Sawaka K., Shima E., Wakamatsu K., 1987, MNRAS, 229, 295
Matsuda T., Sekino N., Shima E., Sawada K., Spruit H. C., 1989, in Meyer F., Duschl W. J., Frank J., Meyer-Hofmeister E., eds, Theory of Accretion Disks. Kluwer, Dordrecht, p. 355
Mayo S. K., Wickramasinghe D. T., Whelan J. A. J., 1980, MNRAS, 193, 793
Papaloizou J. C. B., Lin D. N. C., 1984, ApJ, 285, 818
Papalouizou J. C. B., Pringle J. E., 1977, MNRAS, 181, 441
Papaloizou J. C., Savonije G. J., 1991, MNRAS, 248, 353
Pringle J. E., 1981, ARA&A, 19, 137
Różyczka M., Spruit H. C., 1989, in Meyer F., Duschl W. J., Frank J., Meyer-Hofmeister E., eds, Theory of Accretion Disks. Kluwer, Dordrecht, p. 341
Savonije G. J., Papaloizou J. C., 1983, MNRAS, 207, 685
Sawada K., Matsuda T., Hachisu I., 1986, MNRAS, 219, 75
Sawada K., Matsuda T., Inoue M., Hachisu I., 1987, MNRAS, 224, 307
Shakura N. I., Sunyaev R. A., 1973, A&A, 24, 337
Shu F. H., 1984, In Greenberg R., Brahic A., eds, Planetary rings. Univ. Arizona Press, Tucson, p. 513
Spruit H. C., 1987, A&A, 184, 173
Spruit H. C., 1989, in Meyer F., Duschl W. J., Frank J., Meyer-Hofmeister E., eds, Theory of Accretion Disks. Kluwer, Dordrecht, p. 325
Spruit H. C., Matsuda T., Inoue M., Sawada K., 1987, MNRAS, 229, 517
van Leer B., 1982, Lect. Notes Phys., 170, 505
Warner B., 1976, in Eggleton P. P., Mitton S., Whelan J. A. J., eds, Proc. IAU Symp. 73, Structure and Evolution of Close Binary Stars. Reidel, Dordrecht p. 367
Williams R. E., 1980, ApJ, 235, 939
Williams R. E., Ferguson D. H., 1982, ApJ, 257, 672
Wood J. H., Horne K., Berriman G., Wade R. A., 1989, ApJ, 341, 974